serum albumin and 1.0 mM $NADP^{+}$[3]. The enzyme activity is expressed as nmoles $NADP^{+}$ reduced/min/mg protein. NAG activity was measured using 4-methylumbelliferyl-N-acetyl-β-glucosaminide as substrate[7]. Protein concentration was determined using the biuret reaction[8] with bovine serum albumin as standard.

Results and discussion. The activities of G6PDH and the lysosomal enzyme NAG were measured in the soleus and vastus intermedius both before and for 4 days after eccentric exercise (table). In agreement with Armstrong et al.[3] the activity of G6PDH increased in both muscles after exercise. This increase in G6PDH activity is likely associated with the degeneration-regeneration process[9]. The activity of NAG was also increased in the same muscles following exercise indicating that lysosomal enzymes are also involved in the process of muscle damage and repair. Our observation of increased lysosomal enzyme activity after eccentric exercise substantiates Friden's et al. finding of increased lipofuscin granules in human subjects after eccentric exercise[10]. The maximum increase in G6PDH activity was 296 and 47% in the vastus intermedius and soleus respectively while the increase in NAG activity was only 65 and 30% in the same muscles. Thus while both of these enzymes are good biochemical markers of muscle damage, G6PDH was used in subsequent studies because of its greater responsiveness.

Glucose 6-phosphate dehydrogenase (G6PDH) and N-acetyl-β-glucosaminidase (NAG) activity in muscles of 411 ± 6 g rats

Hours post exercise	Enzyme activity (nmoles/min/mg protein) Vastus intermedius		Soleus	
	G6PDH	NAG	G6PDH	NAG
Control	1.65 ± 0.12	1.96 ± 0.09	4.55 ± 0.24	1.59 ± 0.04
24	1.74 ± 0.11	1.65 ± 0.07	4.85 ± 0.55	1.89 ± 0.09
48	3.18 ± 0.61	2.08 ± 0.15	6.71 ± 0.50*	1.95 ± 0.32*
72	6.54 ± 1.14*	3.23 ± 0.59*	5.48 ± 0.52	2.06 ± 0.11*
96	4.06 ± 0.62	2.28 ± 0.16	4.12 ± 0.19	1.85 ± 0.07

Values are means ± SE for 10 observations. Asterisks indicate the value is statistically different ($p < 0.05$) from the control value.

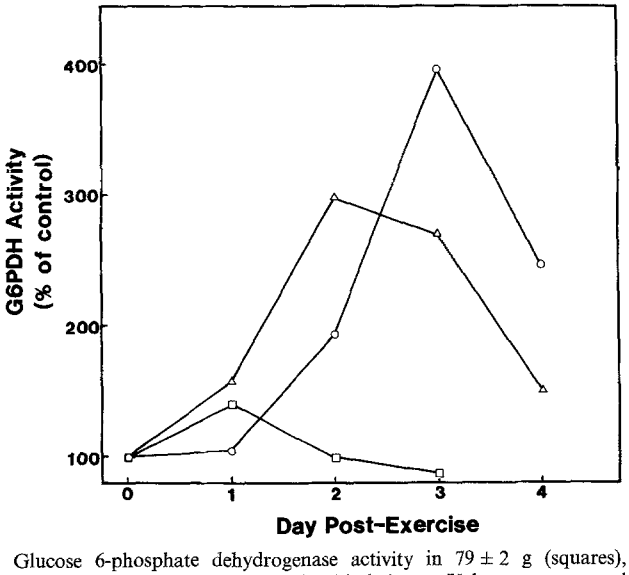

Glucose 6-phosphate dehydrogenase activity in 79 ± 2 g (squares), 269 ± 5 g (triangles), and 411 ± 6 g (circles) rats. Values are expressed as percent of control. The control values were 3.80 ± 0.16, 1.95 ± 0.19, and 1.65 ± 0.12 nmoles/min/mg protein for the 79, 269, and 411 g rats respectively.

The effect of rat size (age) on exercise-induced muscle damage was assessed by measuring the activity of G6PDH in small and medium sized rats as a function of time after exercise and comparing these data to the data from the large rats obtained in our first experiment. The G6PDH activity increased with increasing rat size (fig.). The small rats (79 ± 2 g) showed only a 40% increase while the large rats (411 ± 6 g) which ran at the same intensity for slightly less time had a 296% increase. The medium sized rats (269 ± 5 g) showed an intermediate 197% increase even though they had to be run both longer and faster to achieve the same degree of 'tiredness' as the other two groups. It thus appears that exercise-induced muscle damage increases as the animal gets older and larger.

The time course of the G6PDH activity shows that the maximal increase occurs 1, 2, and 3 days post exercise in the small, medium, and large rats respectively. Since G6PDH is associated with this repair process, it appears that this process is delayed in the larger animals. Thus, it seems that older and larger animals are not only more susceptible to exercise-induced muscle damage, but recover from this damage more slowly than younger and smaller animals.

1 Asmussen, E., Acta rheum. scand. *2* (1956) 109.
2 Komi, P.V., and Viitasalo, J.T., Acta physiol. scand. *100* (1977) 246.
3 Armstrong, R.B., Ogilvie, R.W., and Schwane, J.A., J. appl. Physiol. *54* (1983) 80.
4 Hough, T., Am. J. Physiol. *1* (1902) 76.
5 Friden, J., Sjostrom, M., and Eklblom, B., Experientia *37* (1981) 506.
6 Vihko, V., Salminen, A., and Rantamaki, J., J. appl. Physiol. *47* (1979) 43.
7 Dohm, G.L., Williams, R.H., Kasperek, G.J., and Van Rij, A.M., J. appl. Physiol. *52* (1982) 27.
8 Gornall, A.G., Bardawill, C.J., and David, M.M., J. biol. Chem. *177* (1949) 751.
9 Tullson, P., and Armstrong, R.B., Experientia *37* (1981) 1311.
10 Friden, J., Kjorell, U., and Thornell, L.E., Int. J. Sports Med. *5* (1984) 15.

0014-4754/85/050616-02$1.50 + 0.20/0
© Birkhäuser Verlag Basel, 1985

Supramarginal cells in the rat pituitary cleft revealed by scanning electron microscopy

S. Correr and P.M. Motta

Department of Anatomy, Faculty of Medicine, University of Rome, viale Regina Elena 289, I-00161 Rome (Italy), 23 May 1984

Summary. An unusual cell type consisting of free elements widely scattered over the marginal epithelium of the rat pituitary cleft is revealed by SEM. Most of these supramarginal cells characteristically have irregularly shaped cell bodies from which thin branched processes extend. Supramarginal cells bear resemblances to Kolmer (epiplexus) cells and to supraependymal cells of the brain ventricles. Their ultrastructural features make it probable that supramarginal cells are phagocytes, and can be regarded as scavengers of the cleft. Considering the close topographical association between the hypophysial cleft and the floor or the 3rd ventricle, supramarginal cells may be members of the motile macrophagic Kolmer cells populating the ventricular surfaces of the brain.
Key words. Rat pituitary cleft; scanning electron microscopy; supramarginal cells.

The structure of the pituitary cleft in mammals may be of significance with respect to its close topographical association with the hypothalamo-hypophysial complex[1–3]. Early three-dimensional studies demonstrated that many marginal cells lining the cavity of the cleft possess basal irregular processes. These penetrate between secretory cells of the adenohypophysis and often end in contact with pituitary capillaries and other parenchymal cells[3,4]. A similarity of function between cleft marginal cells and ependymal cells lining the 3rd ventricle, and particularly its recesses, has been suggested[3,5]. This scanning electron microscopic (SEM) study reveals irregularly shaped cells widely scattered over the marginal layer of the rat pituitary cleft. These elements strongly resemble the supraependymal cells found in the 3rd ventricle[6–11].

Materials and methods. Hypophyses of 30 adult albino rats of both sexes were used. After vascular perfusion with 2.5% glutaraldehyde in cacodylate buffer (0.10 M at pH 7.4) the skull of each animal was opened. The hypophyses, carefully removed, were immersed for 12–72 h in a fixative similar to that used for perfusion. In order to scan the entire cleft the pituitaries were partially dissected. Fragments of tissues were washed in the buffer, dehydrated and critical point dried in liquid CO_2 using a Sorvall apparatus. Blocks were mounted with silver paint on metal stubs. Finally the specimens were coated with gold using a sputter coater prior to examination in a Cambridge 150 stereoscan microscope operating at 10–15 kV. For transmission electron microscopy (TEM), control fragments were postfixed in osmium, dehydrated and embedded in Epon 812. The thin sections, stained with uranyl acetate and lead citrate, were viewed in a Zeiss E/M 9A.

Results. Observed under the SEM the rat pituitary cleft was seen to be lined with marginal cells possessing microvilli or cilia. Mostly ciliated cells were found over the caudal part of the cleft. Cells with smooth surfaces and isolated and centrally located cilia were also noted (figs 1–3). Other marginal cells showed a number of apical protrusions such as blebs, ruffles and short microvilli restricted to the margins of the cells[2–5].

Free cells located above the marginal epithelium were found in the rat hypophysial cleft (figs 1–3). These cells – hereafter called supramarginal cells (SMc) – were observed on the surface of both walls of the fissure. Generally SMc occurred singly but occasionally they were in small groups of similar cells (figs 1–3). Some SMc showed a large cell body radiating polymorphic cortical processes and thus assumed a characteristic star shape (figs 1 and 2). Other SMc possessed a roundish, spindle-shaped or triangular cell body from which two or three long thick evaginations emerged (figs 3 and 4). These cells, observed for comparison by TEM, showed an irregularly shaped nucleus. The cytoplasm was provided with polymorphic dense bodies (lysosomes) and vacuoles often containing digested material of unknown nature (figs 3a and 4a).

Furthermore irregularly shaped cells resembling SMc were also observed in wide intercellular and pericapillary spaces. Mostly these cells were in zones of the adenohypophysis close to the marginal layer of the cleft (figs 5 and 5a).

Discussion. Cells attached to the ventricular surface of the choroid plexus of lower vertebrates and mammals were first recognized by Kolmer[12] and have come to be known as Kolmer(epiplexus)cells[13–15].

By parallel TEM and SEM observations Kolmer cells have been

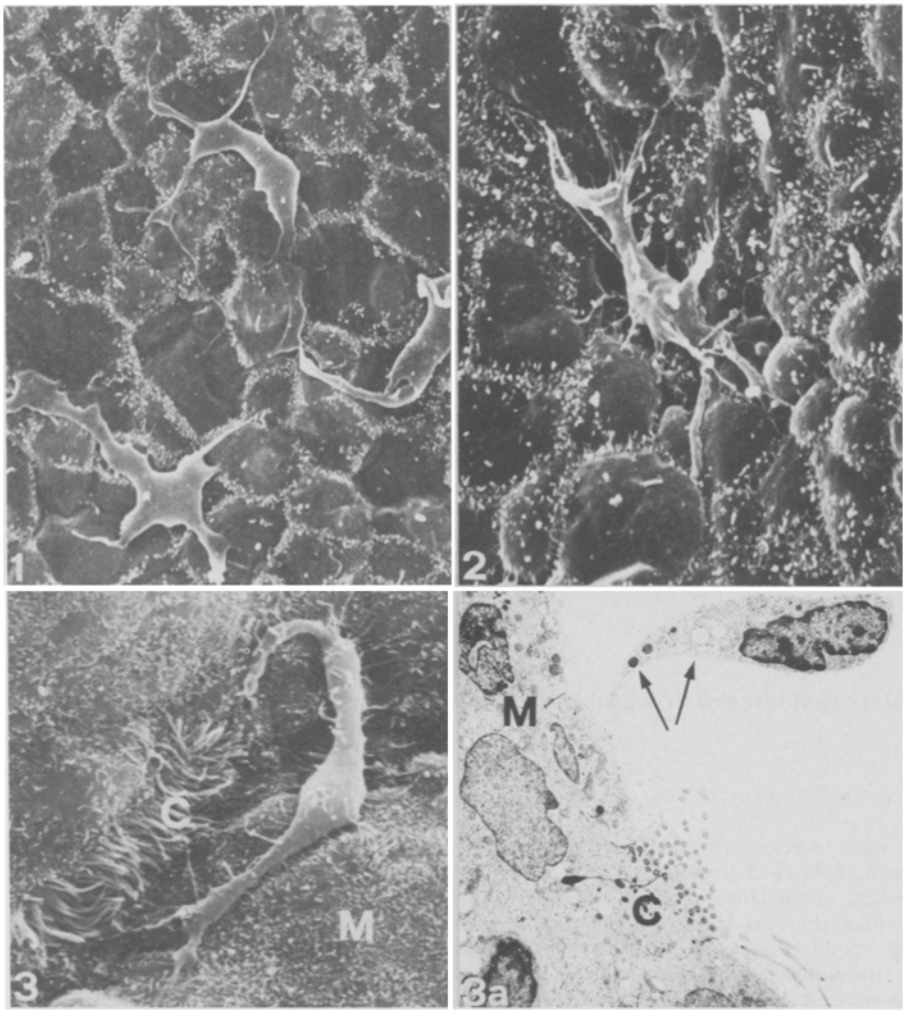

Figures 1 and 2. Stellate supramarginal cells (SMc) distributed over the marginal epithelium of the pituitary cleft. The SMc in figure 2 is partially infolded in a depression of the marginal layer (fig. 1 ×1125; fig. 2 × 1350).

Figures 3 and 3a. Correlated SEM and TEM pictures of SMc. The cells are spindle-shaped and bear pseudopodial processes extending over the microvilli (M) and cilia (C) of the marginal epithelium of the cleft. The SMc of figure 3a shows a cytoplasm containing a number of polymorphic vacuoles and dense bodies of probable lysosomal nature (arrows) (fig. 3, SEM, ×2850; fig. 3a, TEM, × 3450).

identified as macrophages probably derived from blood monocytes[10,11,16,17]. Furthermore, using SEM methods, other cells were usually found along the ependymal walls of the brain ventricles and termed supraependymal cells[6-11]. These elements, closely resembling Kolmer cells, were especially common in the recesses and along the floor of the 3rd ventricle of various mammals[7-11]. Supraependymal cells were generally regarded as macrophages somewhat related to or derived from Kolmer cells[6-11,16-19].

Finally other studies suggested that in some ventricular regions, certain groups of supraependymal cells had a glial structure or were modified neurons[9,11].

In their surface fine features the SMc of the rat pituitary described in this study bear striking resemblances to Kolmer cells and supraependymal cells[6-11,18,19]. The probable phagocytic property of SMc is indicated in these SEM observations by their irregular cell projections similar to those typically displayed by macrophages elsewhere[18-23]. Further, the macrophagic nature of SMc seems to be suggested by the occurrence in the cytoplasm of large phagocytic vacuoles and lysosome-like bodies.

In the light of these results it is reasonable to suggest that SMc are macrophages of possible hematogenous origin which migrated from the hypophysial tissues to the cleft. This origin is likely if we consider that macrophage-like cells, resembling SMc, were also found in close association with the marginal layer of the cleft or in the intercellular and pericapillary spaces of the hypophysis.

Like macrophages in other organs of the body the presence of SMc in the pituitary cleft might depend upon the local physiological demands of the hypophysis. Particularly in the pituitary the phagocytic function of SMc might help to provide a defense barrier and to remove extraneous material accumulated in the cleft as a result of the glandular activity. Moreover, as also postulated for macrophages in different endocrine tissues[24-26], macrophagic SMc may play an important part in modulating the function of the hypophysis and maintaining its hormone secretion.

Finally, another possibility which cannot be ruled out is that SMc arise from detached marginal cells or from the folliculostellate cells of the hypophysis. In fact, particularly these latter have been shown to assume active phagocytic properties under some conditions[27-29].

* Work supported by grants from MPI-60%-193/84

1 Ciocca, D.R., and Gonzales, C.B., Tissue Cell *10* (1978) 725.
2 Ciocca, D.R., Cell Tissue Res. *206* (1981) 139.
3 Correr, S., and Motta, P.M., Cell Tissue Res. *215* (1981) 515.
4 Correr, S., and Motta, P.M., Biomed. Res. *2* (suppl.) (1981) 109.
5 Barberini, F., and Correr, S., in: Ultrastructure of Endocrine Cells and Tissues, p. 57. Ed. P.M. Motta. M. Nijhoff Publ., Boston/The Hague 1984.
6 Allen, D.J., J. comp. Neurol. *161* (1975) 197.
7 Coates, P.W., Am. J. Anat. *136* (1973) 533.
8 Mestres, P., and Breipohl, W., Cell Tissue Res. *168* (1976) 303.
9 Scott, D.E., Paull, W.K., and Sheridan, M.N., Int. Rev. Cytol. *37* (1974) 349.
10 Hosoya, Y., and Fujita, T., Archvm histol. jap. *35* (1973) 133.
11 Seymour, R.M., and Berry, M., in: Biomedical Research Applications of SEM, vol. 1, p. 127. Eds G.M. Hodges and R.C. Hallowes. Academic Press, London/New York 1979.
12 Kolmer, W., Anat. Anz. *54* (1921) 15.

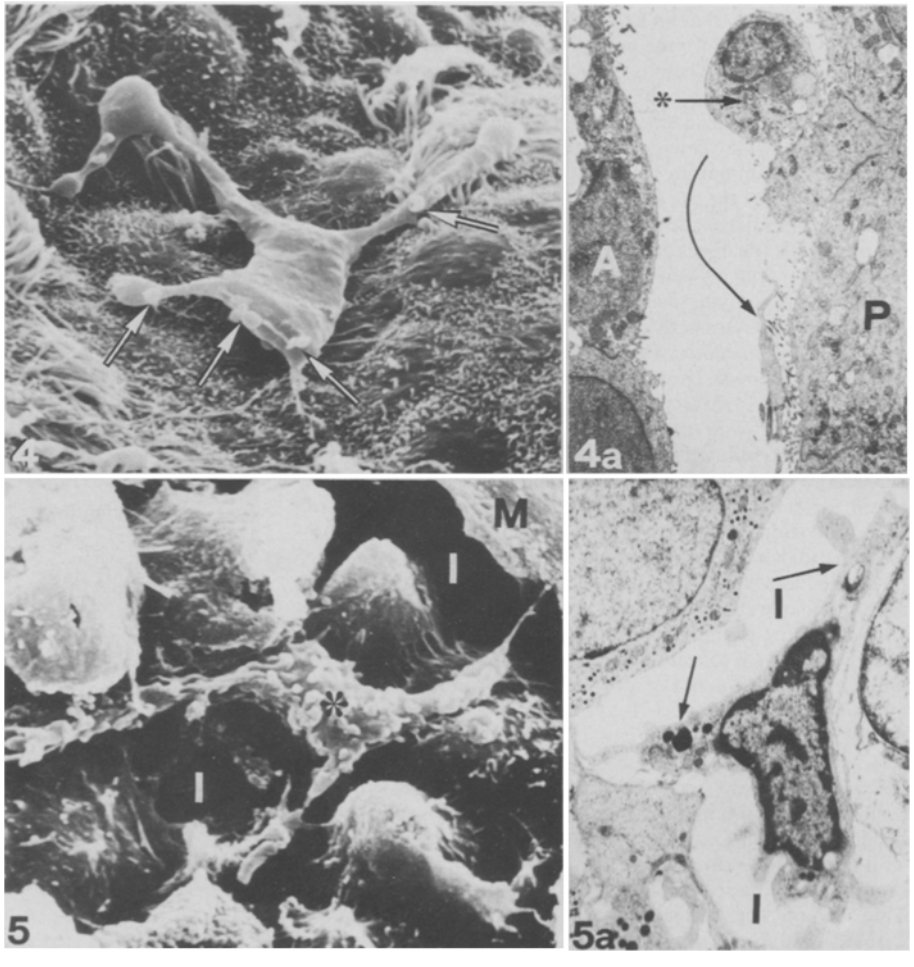

Figures 4 and 4a. Correlated SEM and TEM of SMc. Long pseudopodial evaginations emerge from the cell body and extend over the marginal layer of the cleft. A number of pieces of debris adhere to the surface of these evaginations (small arrows in fig. 4). The SMc present in figure 4a has a roundish cell body and a cytoplasm filled with polymorphic phagocytic vacuoles (arrow plus asterisk). A cytoplasmic process extends from the SMc (arrow). Anterior (A) and posterior (P) wall of the cleft (fig. 4, SEM, ×3375; fig. 4a, TEM, ×3600).

Figures 5 and 5a. SEM and TEM micrographs of multipolar cells (asterisk) with ultrastructural features similar to SMc. These elements are located in intercellular spaces (I) of the adenohypophysis close to the flattened marginal cells (M) of the anterior wall of the cleft. A number of dense bodies (lysosomes) and sparse vacuoles are evident in the cytoplasm of the cell in figure 5a (fig. 5, SEM, ×3000; fig. 5a, TEM, × 3375).

13 Vialli, M., Riv. sper. Freniat. *54* (1930) 120, 351.
14 Scharrer, E., Z. Zellforsch. *23* (1936) 244.
15 Ariens-Kappers, G., Z. Anat. Entw. Gesch. *117* (1953) 1.
16 Tennyson, V.M., and Pappas, G.D., J. comp. Neurol. *123* (1964) 379.
17 Carpenter, S.J., McCarthy, L.E., and Borison, H.L., Z. Zellforsch. *110* (1970) 471.
18 Sturrock, R.R., J. Anat. *136* (1983) 761.
19 Ling, E.A., J. Anat. *137* (1983) 645.
20 Albrecht, R.M., and Bleier, R., Scanning Electron Microscopy *3* (1979) 55.
21 Motta, P.M., Cell Tissue Res. *164* (1975) 371.
22 Parakkal, P., Pinto, J., and Hanifin, H.M., J. Ultrastruct. Res. *48* (1974) 216.
23 Polliack, A., and Gordon, S., Lab. Invest. *33* (1975) 469.
24 Kirsch, T.M., Friedman, A.C., Vogel, R.L., and Flickinger, G.L., Biol. Rev. *25* (1981) 629.
25 Motta, P.M., Muto, M., and Fujita, T., Cell Tissue Res. *196* (1979) 23.
26 Miller, S.C., Bowman, B., and Rowland, H.D., Am. J. Anat. *168* (1983) 1.
27 Dingemans, K.P., and Feltkamp, C.P., Z. Zellforsch. *124* (1972) 387.
28 Shiotani, Y., Cell Tissue Res. *213* (1980) 237.
29 Vila-Porcile, E., and Olivier, L., in: Ultrastructure of Endocrine Cells and Tissues, p. 64. Ed. P.M. Motta. M. Nijhoff Publ., Boston/The Hague 1984.

0014-4754/85/050617-04$1.50 + 0.20/0
© Birkhäuser Verlag Basel, 1985

Colloidal carbon as a multilevel marker for experimental lesions

L. C. Triarhou and M. del Cerro

Center for Brain Research, University of Rochester School of Medicine and Dentistry, Rochester (New York 14642, USA), 30 May 1984

Summary. The use of colloidal carbon for the anatomical marking of experimental lesions is proposed. Visualization of the lesion site may be readily performed through this procedure at the macroscopic, light microscopic, and ultrastructural levels in the same specimen. The chemical inertness of the marker and its relative permanency greatly add to its usefulness.
Key words. Carbon; central nervous system; demyelinating diseases; electron microscopy; injections; light microscopy; lysophosphatidylcholines.

There is a modern trend in neuroscience to place minute lesions, or microinjections, into the nervous system to serve a variety of experimental goals. There is often a need to identify those foci sequentially at macroscopic, light and electron microscopic levels. A difficulty in localizing the lesion while preparing tissues for histopathology may emerge from the small size of the locus and the lack of inflammatory reaction.

This note reports the use of colloidal carbon as a morphological marker for multilevel identification of such injection sites, using as an example the injection of lysolecithin into the spinal cord of experimental animals which has proven to be an extremely useful model for studying demyelination and remyelination in the central nervous system[1,2].

Materials and methods. The colloidal carbon suspension was prepared as follows: Three to 5 ml of India ink ('Pelikan' special ink, batch C11/1431A) were dialyzed against distilled water for 48–72 h through a Spectrapor semipermeable membrane (Spectrum Medical Industries, Inc., Los Angeles, CA 90054) with 12,000 MW cut-off. The suspension could be stored in the refrigerator for many months. To mark the site of lysolecithin injections, one drop of dialyzed ink was added to 1 ml of 1% lysophosphatidylcholine solution. The surgical operation has been described elsewhere[2]. This procedure produces well-localized, reproducible lesions of known age.The size of the lesion may vary according to the amount of lysolecithin injected. Injection of 2 µl of a 1% lysolecithin solution into the lower thoracic or upper lumbar region of the rat spinal cord produces a focal area of primary demyelination of approximately 0.4 mm diameter. At different postoperative times, intracardiac perfusion fixation was performed and spinal cords were dissected and inspected macroscopically to locate the injection sites. Subsequently, tissue blocks containing the lesions were processed and embedded in Epon. One micrometer thick sections were stained with Stevenel blue for light microscopy[3] or reacted with antiserum to myelin basic protein (MBP) for immunocytochemistry[4]. Thin sections were stained with lead citrate for electron microscopy[5].

Results. The injection tracks in lysolecithin-injected animals appeared macroscopically as straight black lines in the ventrolateral white matter of the spinal cord (fig. 1). The lesions remained labeled for at least 70 postoperative days, the longest survival time allowed in this series.

Light microscopy of 1 µm thick sections reacted with anti-MBP serum revealed reaction in the healthy, but not in the demyelinated, area. The presence of carbon could be readily detected within the affected tissue (fig. 2). At later stages, when remyelination took place (fig. 3), carbon tattoo remained as an indicator of the original site of lysolecithin injection.

The removal of carbon took place slowly, primarily by the action of invading phagocytes. The electron micrograph of figure 4 depicts part of a macrophage actively involved in the phagocytosis of both myelin debris and colloidal carbon.

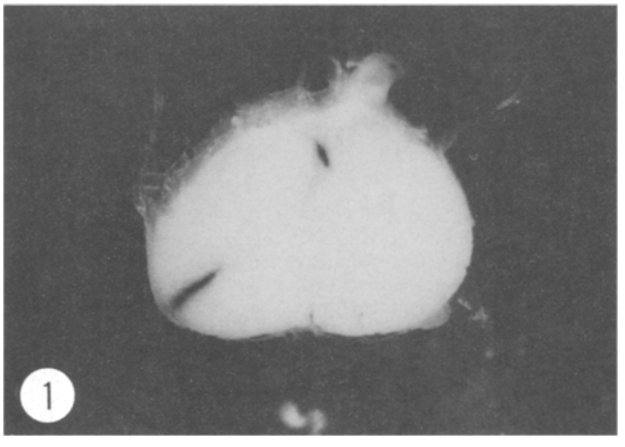

Figure 1. Cross section of an unstained spinal cord block, with the site of lysolecithin injection marked with carbon. × 15.